

Characterization of Co-Fe Magnetic Films Fabricated by Galvano-Static Electrodeposition

Z. Ghaferi^{1,2*}, S. Sharafi¹ and M. E. Bahrololoom³

* ghaferi_z@yahoo.com

Received: December 2016

Accepted: April 2017

¹ Department of Material Science and Engineering, Faculty of Engineering, Shahid Bahonar University of Kerman, Kerman, Iran.

² Young Researchers Society, ShahidBahonar University of Kerman, Kerman, Iran.

³ Department of Material Science and Engineering, Faculty of Engineering, Shiraz University, Shiraz, Iran.

DOI: 10.22068/ijmse.14.2.60

Abstract: In this research, nanocrystalline Co-Fe coatings were electrodeposited on copper substrate. The influence of current density on different properties of the films at two pH levels was investigated. All the coatings showed nodular structure with rougher morphology at higher current densities. Due to anomalous deposition at higher current density, the amount of iron content increased and reached its maximum value at about 50 wt.% for the coating obtained from pH 5. X-ray diffraction patterns showed hcp structure as the dominant phase. However, by increasing current density at lower pH value, a double phase structure containing fcc+hcp phases was detected. It was observed that current density has a positive effect on grain refinement. However, coarser grains would obtain at lower pH value. Microhardness measurements showed that, there is a direct relationship between grain size and microhardness. Moreover, microstructure in double phase structure films can influence microhardness more dominantly. Vibrating sample magnetometer (VSM) measurements indicated that the saturation magnetic is proportion to deposited iron content and reached its maximum value at about 1512 emu/cm³. It was cleared that grain size, phase structure and chemical composition can affect coercivity of the films effectively.

Keywords: Co-Fe, Current density, Microstructure, Microhardness, Magnetic property.

1. INTRODUCTION

Electrodeposited Co-Fe alloys are important engineering materials used in different industries including communication devices, sensors, actuators, printed circuit boards and magnetic recording heads [1-3]. These materials have high saturation magnetization and Curie temperature, high permeability, low eddy current loss and thermal stability [1, 2].

Many investigations have been carried out for development of these coatings. The influence of homogeneous magnetic fields on internal stress, microstructure, roughness and chemical composition of Co-Fe alloys have been examined by Koza and co-workers [4]. Kim et al. [5] have found that current efficiency obtained from chloride baths is higher than that obtained from sulphate electrolytes and this parameter is decreased by increasing Fe²⁺ concentration [6].

It has been reported that the presence of internal stress which causes microcracks

formation during electrodeposition process affects corrosion resistance, magnetic and mechanical properties of the films [7, 8]. The internal stress is originated from grain size refinement, higher film thickness, increasing iron content and/or fierce hydrogen evolution during electrodeposition process [8-11].

Kockar and co-workers [12] investigated the magnetic properties of Co-Fe alloys as a function of electrolyte pH. Their observations showed that all the films have anisotropic magnetoresistance. However, saturation magnetization of the films reaches its maximum value at about 1597 emu/cm³ at lower pH electrolyte. Lu et al. [13] demonstrated that chemical composition, microstructure and thus magnetic properties of FeCo alloy coatings are influenced by deposition temperature. Their observations showed that Fe content decreased by increasing bath temperature. However, grain size of two phase structure coatings is lower than that obtained from single phase solid solution which is referred

to competitive nucleation and growth of the two phases [13]. Mehrizi et al. [3] have also reported the same results. Despite fine magnetic properties, these alloys have high coercivity which causes energy consumption and reduces lifetime of the devices [3, 14-16]. To overcome this problem, reducing the grain size in nanometer scale is recommended [3].

Among different deposition techniques used for fabricating nanostructured materials, electrodeposition can be a good candidate due to its numerous advantages. The most important positive points of this technique are high quality deposition coatings, rapid production at room temperature, low cost and easy control process. In addition, this procedure does not require any vacuum system and secondary processing steps [9, 17, 18].

Although fine magnetic properties and good mechanical features require for fabricating write heads, lower attentions have been devoted for development of these properties as a function of current density [2, 4, 9, 11-13, 15, 19-21]. Thus in the present work, nanocrystalline Co-Fe alloys were fabricated by electrodeposition technique. The influence of current density on chemical composition, microstructure, magnetic property and microhardness of the films at two pH levels

was investigated.

2. EXPERIMENTAL DETAILS

2. 1. Materials

Rectangular copper samples with 1 cm² surface area were used as cathode. This metal was selected due to easy surface preparation, more accessible, non-magnetic property and high electrical conductivity. Prior to the deposition process, the mechanical polishing of the samples was done up to 3000 grade abrasive paper. Electrodeposition was performed using a digital coulometer (BHP 2056) without agitation and a 430 stainless steel sheet was used as anode surface. The composition of the baths and operating parameters are shown in Table 1. The pH values were adjusted by using dilute H₂SO₄ or NaOH solutions.

2. 2. Methods

The surface morphology and compositional analysis of the coatings were studied by a scanning electron microscope (SEM model WEGA/TESCAN) coupled with an energy dispersive spectrometer (EDS) respectively. To

Table 1. chemical composition of the baths and some deposition conditions for Co-Fe alloys

| Bath composition | Concentration (M) |
|--------------------------------------------------|-------------------|
| CoSO ₄ . 7H ₂ O | 0.20 |
| FeSO ₄ . 7H ₂ O | 0.20 |
| H ₃ BO ₃ | 0.40 |
| Na ₂ SO ₄ | 0.70 |
| L-ascorbic acid | 0.05 |
| Electrodeposition parameters | value |
| Current density (mA/cm ²) | 10, 20, 35, 50 |
| pH | 3, 5 |
| Temperature (°C) | 25 |
| Electric charge passed (colomb/cm ²) | 50 |

evaluate the film thickness, a Motic optical microscope was used. The structural analysis and the grain size measurement were carried out by X-ray diffraction (XRD) technique using Cu K α radiation (BRUKER/D8 ADVANCED diffractometer, 30 kV-30 mA) and the results were interpreted by X-pert high score software. The grain size was calculated from broadening of the cobalt (101) peak using the Scherrer equation [22]:

$$d=0.9 \lambda / \beta \cos\theta \quad (1)$$

where λ , β and θ are the wavelength of copper ($\lambda = 1.5406 \text{ \AA}$), the full width at half-maximum of the peak (FWHM) and the diffraction angle respectively. The scan was done between 40–100 degrees with a step size of about 0.03 degrees. Microhardness of the alloy coatings was determined by using a Koopa MH1 microhardness tester at a constant load of about 15 g for 10 s. The reported values were the

average number of five random points on the surface of each coating. The magnetic hysteresis loops were obtained with a vibrating sample magnetometer (Meghnatis Daghigh Kavir Co. Iran). The samples were prepared by using a very thin copper foil with 0.5 cm \times 0.5 cm dimensions. Magnetic measurements were performed at room temperature and a parallel magnetic field of about $\pm 2000 \text{ Oe}$ was applied to the film surface.

3. RESULT AND DISCUSSION

3. 1. Chemical Composition and Surface Morphology

Figs. 1(a–d) and 2(a–d) show SEM images of the coatings obtained from different current densities for both pH values. As seen, a nodular morphology is observed for all current densities. Since the rate of nucleation and growth is proportion to current density [23], the number of nodules increases at higher current density which causes rougher morphology under this condition. Similar results have been also reported

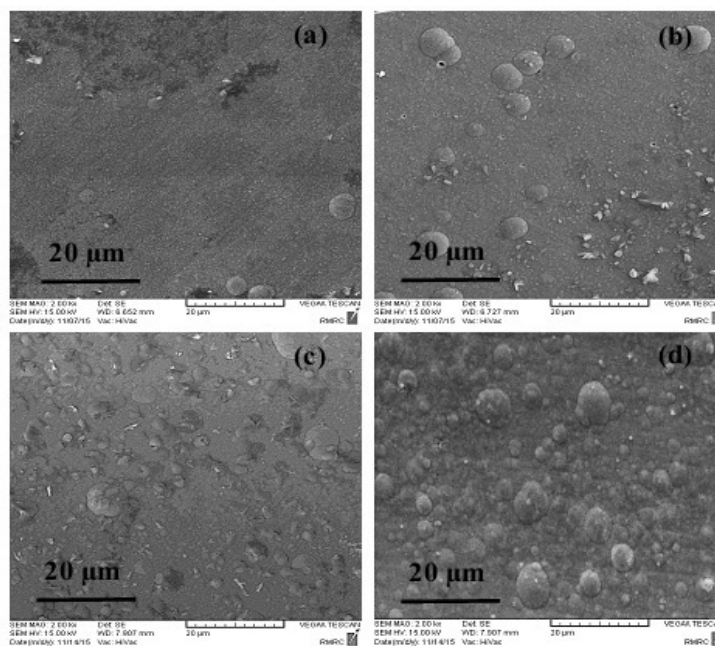


Fig. 1. SEM images of Co-Fe alloy coatings obtained from different current densities and pH=5. The labels (a)-(d) represent current densities $i = 10, 20, 35$ and 50 mA/cm^2 , respectively.

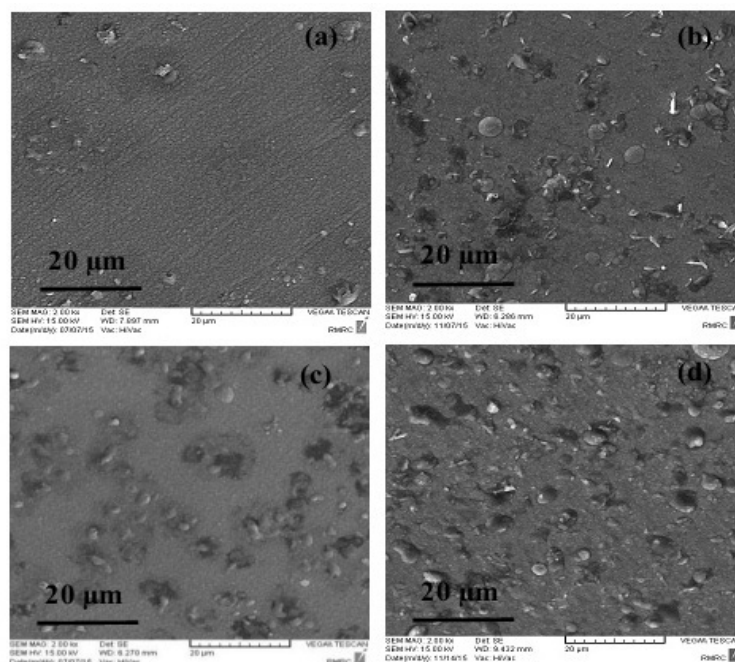


Fig. 2. SEM images of Co-Fe alloy coatings obtained from different current densities and pH=3. The labels (a)-(d) represent current densities $i=10, 20, 35$ and 50 mA/cm^2 , respectively.

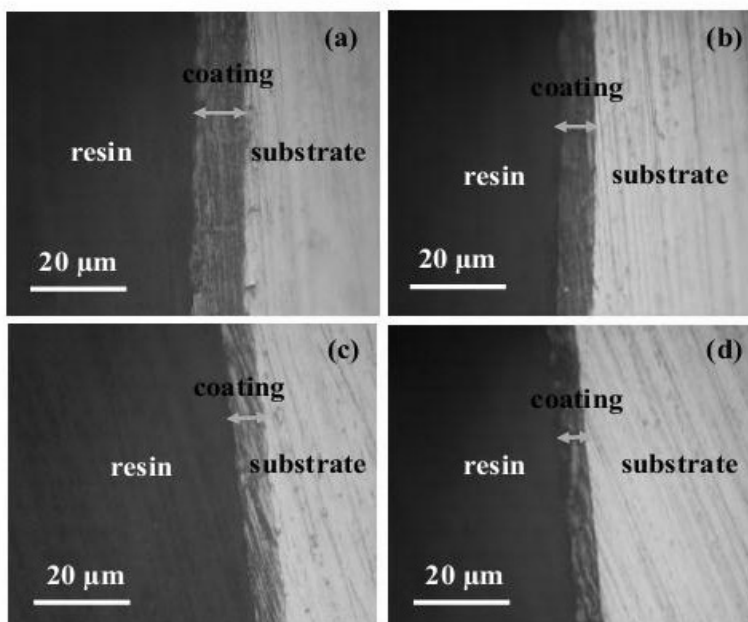


Fig. 3. Optical microscopy images from the cross section of the coatings obtained from different current densities and pH values. The labels (a)-(d) are related to ($i=10 \text{ mA/cm}^2$, pH 5), ($i=50 \text{ mA/cm}^2$, pH 5), ($i=10 \text{ mA/cm}^2$, pH 3), ($i=50 \text{ mA/cm}^2$, pH 3) respectively.

Table 2. EDS, XRD and VSM data for the coatings obtained from pH=5.

| Current density (mA/cm ²) | Fe (wt. %) | Co (wt. %) | Grain size (nm) | Phase structure | M _s (emu/cm ³) | H _c (Oe) |
|------------------------------------------|------------|------------|--------------------|--------------------|------------------------------------------|---------------------|
| 10 | 35 | 65 | 19 | hcp | 1050 | 52 |
| 20 | 44 | 56 | 15 | hcp | 1276 | 41 |
| 35 | 46 | 54 | 12 | hcp | 1348 | 36 |
| 50 | 50 | 50 | 8 | hcp | 1512 | 22 |

Table 3. EDS, XRD and VSM data for the coatings obtained from pH=3.

| Current density (mA/cm ²) | Fe (wt. %) | Co (wt. %) | Grain size (nm) | Phase structure | M _s (emu/cm ³) | H _c (Oe) |
|------------------------------------------|------------|------------|--------------------|--------------------|------------------------------------------|---------------------|
| 10 | 29 | 71 | 25 | hcp | 997 | 46 |
| 20 | 36 | 64 | 19 | hcp | 1087 | 31 |
| 35 | 42 | 58 | 16 | hcp+fcc | 1117 | 24 |
| 50 | 45 | 55 | 11 | hcp+fcc | 1162 | 16 |

previously [24]. Optical microscopy images from the cross section of the coatings are shown in Fig. 3 (a-d). It has been reported that, film thickness is theoretically proportion to the electric charge passed during electrodeposition process [3]. Although, the electric charge was kept constant at 50 colomb/cm², the real film thickness was not the same. In fact, the film thickness was decreased by increasing current density and this effect became more intense at lower pH value. The difference in film thickness is related to fierce hydrogen evolution and lower current efficiency which occurs at these conditions. These results were also confirmed by other researchers [25-28].

Tables 2 and 3 show chemical composition of the coatings obtained from different current densities for both pH values. The results were reported in weight percentage using EDS analysis. As seen, by increasing current density the amount of iron content was increased which

indicates that deposition tends to anomalous fashion under this condition. This expression is used to preferential deposition of the less noble metal compared to the more noble one [10, 18, 27, 29]. To clarify this feature, it must be mentioned that by increasing current density, hydrogen evolution takes place more rapidly at the cathode surface which causes higher pH values near its surface [27]. However, hydroxide ions are dominated species at this condition and the competition adsorption of metal hydroxides causes anomalous deposition [27]. According to Qiang et al. [21] the adsorption tendency of cobalt hydroxide is lower than iron one, which causes higher deposited iron in this condition. This effect became more intense at higher pH electrolytes [25].

3. 2. Structural Characterization

XRD patterns of the coatings as a function of current density for two pH levels are shown in Fig. 4. As seen before, EDS analysis confirmed the existence of iron in the coatings but no iron peaks were seen in the XRD spectra. It means that iron was substituted in the cobalt matrix and thus only cobalt structure as the solvent was detected. Similar results have been also reported by other researchers [8, 17, 24, 25, 30, 31].

It has been reported that cobalt has two allotropic structures containing high temperature fcc and low temperature hcp phases. This transition takes place at around 695 K [8]. During electrodeposition, there is not enough time for arrangement of atoms on regular lattice sites. Thus, non-equilibrium phases can be formed during electrodeposition process [13, 24].

As seen in Fig. 4 (a), it is clear that the peaks diffracted from the coatings deposited from different current densities at pH 5 are due to cobalt hcp structure. According to Fig. 4(b), the structure of the coatings obtained from lower current densities was also the same. However, by increasing current density at pH 3, a double phase structure of cobalt containing hcp+fcc phases became evident. Similar results have been also reported by Sakita et al. [10]. According to Nakahara et al. [32], co-deposition of atomic hydrogen with cobalt ions increases the density of faults in hcp structure and thus a metastable fcc phase was detected. It has been reported that lower pH values and/or higher current densities make suitable conditions for deposition of fcc structure [31].

The average grain size of the coatings was calculated by Scherrer equation and the results are summarized in Tables 2 and 3. It has been reported that current density has two contrary effects on the grain size of the coatings. Firstly, by increasing this parameter, surface diffusion of ad-ions to the active growing sites is increased and thus larger grain size would be obtained at this condition. Secondly, by increasing current density, nucleation rate (J) is promoted and thus finer grains would be acquired based on the following equation [23, 26]:

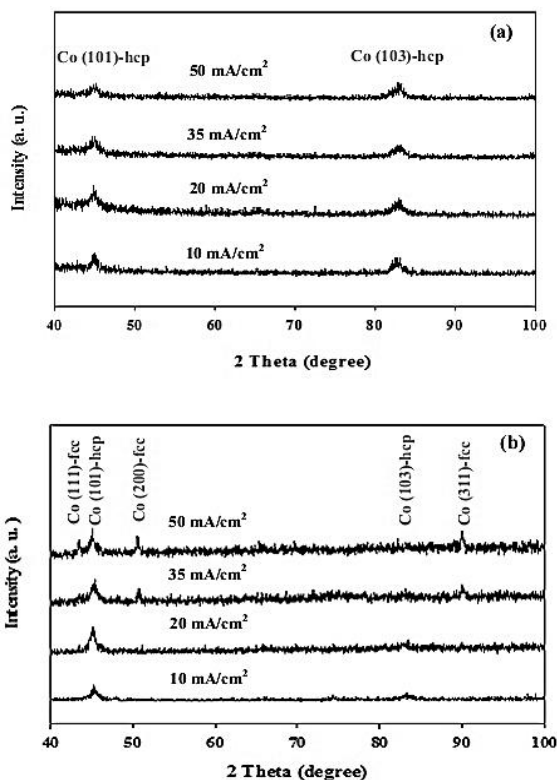


Fig. 4. XRD patterns for Co-Fe alloy coatings obtained from different current densities for (a) pH=5 and (b) pH=3.

$$\lg J = A - \frac{B}{|\Delta\phi|} \quad (2)$$

where A and B are constant and $\Delta\phi$ is the modulus of overpotential. By referring to Tables 2 and 3, it seems that regardless of the electrolyte pH, nucleation rate overcomes the grain growth at higher current densities and thus finer grains would be obtained at this condition. However, the coatings deposited from pH=3 have coarser grains compared to those obtained from the higher pH value. To determine this feature, it can be assumed that hydrogen reduction blocks the nucleation sites more conveniently and this leads to larger grains at lower pH value.

4. MICROHARDNESS OF THE COATINGS

It has been reported that chemical composition, surface defects, crystal orientation,

grain size and phase structure can affect microhardness effectively [8, 24, 25, 31, 34–38]. Figure 5 shows microhardness of the coatings as a function of current density for both pH values. As seen, microhardness of the coatings obtained from pH 5 is higher than those obtained from pH 3 initially. This effect may be due to solid solution hardening and higher iron content deposited at pH 5. However, a significant increase in microhardness value for the coatings obtained from pH 3 at higher current densities is related to a double phase structure coatings formed at this condition. Similar results were also reported by other researchers [9, 36].

The strengthening of polycrystalline materials by grain size refinement can be explained by the Hall-Petch equation [38, 39]:

$$H=H_0+kd^{-0.5} \quad (3)$$

where H_0 is hardness constant, k is a constant and d is the diameter of grains which is determined by XRD technique. In this model, grain boundaries act as obstacles to dislocations movement [38]. As seen from Fig. 5, microhardness of the coatings obtained from pH 5 has descending

trend at higher current densities. It means that the strengthening of material through grain refinement deviates from the normal Hall-Petch equation. This softening effect is related to very small grain size which makes more triple junctions, intercrystalline volume fraction and diffusional creep as reported previously [9, 19, 38]. It has been reported that the deviation from Hall-Petch equation for Co-Fe alloy coatings takes place at around 20 nm grain size [9] which is higher than the reported value in the present investigation.

5. MAGNETIC PROPERTY

Figure 6 illustrates the hysteresis loops of the coatings and the results are summarized in Tables 2 and 3. It has been reported that chemical composition is the main factor responsible for magnetization changes [3, 5, 19]. Since, iron has the highest magnetization compared to other magnetic materials, the variation in this parameter is proportion to deposited iron content [40]. As seen from the mentioned tables, coercivity was decreased at higher current densities. However, the variation in this parameter is related to many factors such as

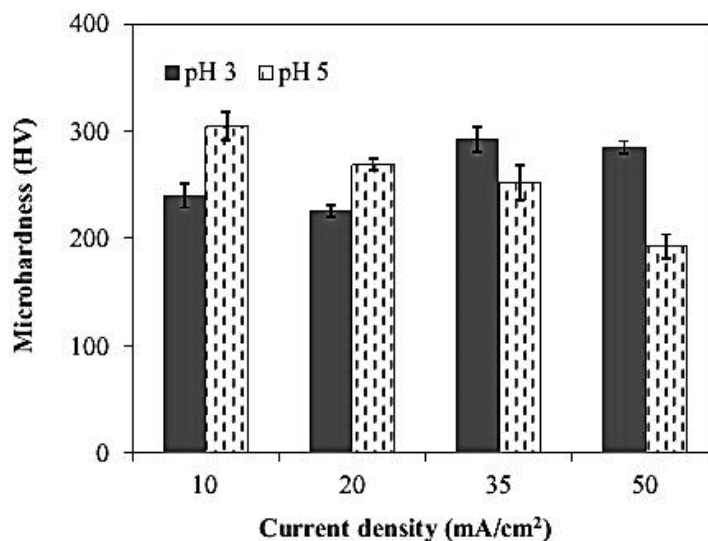


Fig. 5. Microhardness and its error bar for Co-Fe alloy coatings.

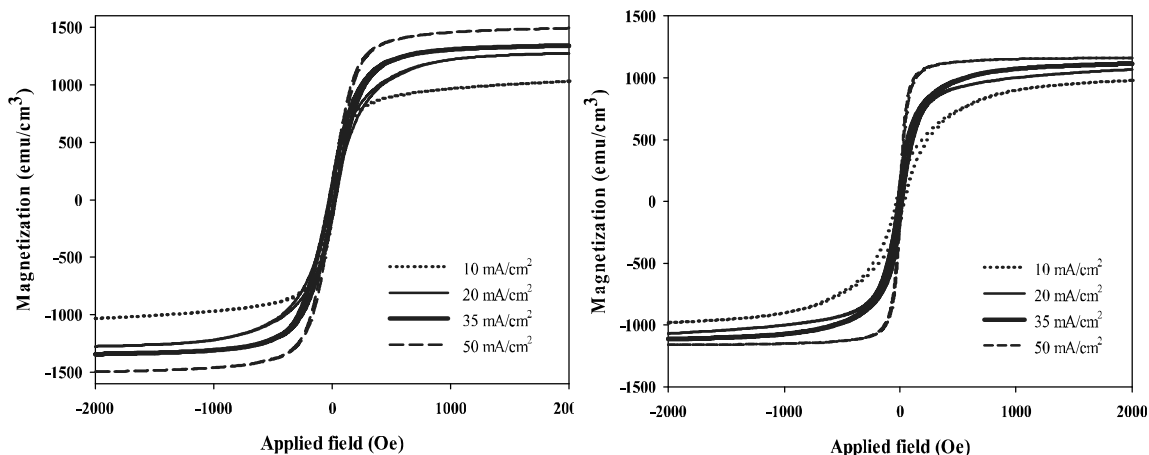


Fig. 6. Hysteresis loops of the coatings obtained from different current densities for (a) pH=5 and (b) pH=3.

chemical composition, surface defects, phase structure, thickness and grain size of the coatings effectively [16, 19, 26].

Based on some documents [41-43], increasing the volume fraction of grain boundaries through grain refinement prevents the domain walls movement and thus higher coercivity would be obtained at this condition. The coercivity is expressed as the following equation [8, 41-43]:

$$H_c \sim 3 \sqrt{\frac{kT_c K_1}{aM_s}} \frac{1}{D} \quad (4)$$

where H_c is the coercivity, D the crystallite size, M_s the saturation magnetization, K_1 the magnetocrystalline anisotropy, T_c the Curie temperature, k the Boltzmann constant and a the lattice constant. However, by decreasing the grain size smaller than magnetic exchange length (L_{ex}) which is approximately of the order of tens nanometers, the domain wall effect is eliminated and the exchange interaction of the grains makes the magnetization vectors more parallel to each other [44]. Thus, coercivity can be determined by the following equation [3, 41-43, 45]:

$$H_c \sim \frac{P_c D^6 K_1^4}{\mu_0 M_s A^3} \quad (5)$$

where P_c is a constant of the order of unity, μ_0 the permeability of free space and A the exchange stiffness constant. The magnetic exchange length is defined as the following equation which is approximately 40 nm for CoFe alloys [3, 41-43, 45]:

$$L_{ex} = \sqrt{\frac{A}{K_1}} \quad (6)$$

As seen previously, grain size of the coatings decreased by increasing current density. Since, the average grain size in this investigation is lower than magnetic exchange length (40 nm), the reduction in this parameter can lead to lower coercivity according to equation 5. It must be mentioned that chemical composition can also affect coercivity of the films effectively. It has been reported that cobalt has higher coercivity compared to other magnetic materials [40]. So the higher cobalt content which was deposited at lower current densities can lead to lower coercivity. Tian et al. [26] have also reported the same results. As seen in previous sections, higher current density and lower pH value provided suitable condition for deposition of fcc phase. It has been reported that fcc phase has lower magnetic anisotropy compared to hcp one which made lower coercivity at this condition [47]. These results are in good agreement with the results obtained here.

6. CONCLUSION

In this research, nanocrystalline Co-Fe alloy coatings were prepared by electrodeposition technique. The results showed that by increasing current densities and/or pH value, deposition tends to anomalous fashion and higher iron content would deposit at these conditions. By considering XRD data, it was demonstrated that lower grain size deposits at higher current densities. Furthermore, lower pH values and higher current densities cause suitable situations for deposition of fcc+hcp structure compared to hcp one. Microhardness of the coatings reached its maximum value at about 300 HV. VSM results confirmed that saturation magnetization of the coatings is proportion to deposited iron content and reaches its maximum value at about 1512 emu/cm³. However, coercivity was changed by chemical composition, microstructure and grain size of the coatings.

REFERENCES

1. Aguirre, M. del C., Fariás, E., Abraham, J. and Urreta, S. E., "Co_{100-x}Fe_x magnetic thick films prepared by electrodeposition", *J. Alloys Compd.* 2015, 627, 393–401.
2. Lu, W., Jia, M., Ling, M., Xu, Y., Shi, J., Fang, X., Song, Y. and Li, X., "Phase evolution and magnetic properties of FeCo films electrodeposited at different temperatures", *J. Alloys Compd.* 2015, 637, 552–556.
3. Mehrizi, S., Heydarzadeh Sohi, M. and Seyyed Ebrahimi, S. A., "Study of microstructure and magnetic properties of electrodeposited nanocrystalline CoFeNiCu thin films", *Surf. Coat. Technol.* 2011, 205, 4757–4763.
4. Koza, J. A., Karnbach, F., Uhlemann, M., McCord, J., Mickel, C., Gebert, A., Baunack, S. and Schultz, L., "Electrocrystallisation of CoFe alloys under the influence of external homogeneous magnetic fields—Properties of deposited thin films", *Electrochim. Acta* 2010, 55, 819–831.
5. Kim, D., Park, D. Y., Yoo, B. Y., Sumodjo, P. T. A. and Myung, N. V., "Magnetic properties of nanocrystalline iron group thin film alloys electrodeposited from sulfate and chloride baths", *Electrochim. Acta* 2003, 48, 819–830.
6. Tabakovic, I., Riemer, S., Jayaraju, N., Venkatasamy, V., Gong, J., "Relationship of Fe²⁺ concentration in solution and current efficiency in electrodeposition of CoFe films", *Electrochim. Acta* 2011, 58, 25–32.
7. Ghaziof, S., Golozar, M. A., Raeissi, K., "Characterization of as-deposited and annealed Cr–C alloy coatings produced from a trivalent chromium bath", *J. Alloys Compd.* 2010, 496, 164–168.
8. Ghaferi, Z., Sharafi, S., Bahrololoom, M. E., "Effect of current density and bath composition on crystalline structure and magnetic properties of electrodeposited FeCoW alloy", *Appl. Surf. Sci.* 2015, 355, 766–773.
9. Nik Rozlin, N. M. and Alfantazi, A. M., "Nanocrystalline cobalt–iron alloy: Synthesis and characterization", *Mater. Sci. Eng. A* 2012, 550, 388–394.
10. Sakita, A. M. P., Passamani, E. C., Kumar, H., Cornejo, D. R., Fugivara, C. S., Noce, R. D. and Benedetti, A. V., "Influence of current density on crystalline structure and magnetic properties of electrodeposited Co-rich CoNiW alloys", *Mater. Chem. Phys.* 2013, 141, 576e581.
11. Shao, I., Romankiw, L.T. and Bonhote, C., "Stress in electrodeposited CoFe alloy films", *J. Cryst. Growth* 2010, 312, 1262–1266.
12. Kockar, H., Alper, M., Sahin, T. and Karaagac, O., "Role of electrolyte pH on structural and magnetic properties of Co–Fe films", *J. Magn. Mater.* 2010, 322, 1095–1097.
13. Lu, W., Huang, P., He, C. and Yan, B., "Compositional and Structural Analysis of FeCo Films electrodeposited at different Temperatures", *Int. J. Electrochem. Sci.* 2012, 7, 12262 – 12269.
14. Kumari, T. P., Raja, M. M., A. Kumar, S. Srinath, S. V. Kamat, "Effect of thickness on structure, microstructure, residual stress and soft magnetic properties of DC sputtered Fe₆₅Co₃₅ soft magnetic thin films", *J. Magn. Mater.* 2014, 365, 93–99.
15. Ricq, L., Lallemand, F., Gigandet, M. P. and Pagetti, J., "Influence of sodium saccharin on the electrodeposition and characterization of CoFe magnetic film", *Surf. Coat. Technol.* 2001, 138, 278–283.
16. Karpuz, A., Kockar, H., Alper, M., "Effect of film thickness on properties of electrodeposited

- Ni–Co films”, *Appl. Surf. Sci.* 2012, 258, 5046–5051.
17. Della Noce, R., Benedetti, A. V., Magnani, M., Passamani, E. C., Kumar, H., Cornejo, D. R. and Ospina, C. A., “Structural, morphological and magnetic characterization of electrodeposited Co–Fe–W alloys”, *J. Alloys Compd.* 2014, 611, 243–248.
 18. Karpuz, A., Kockar, H., Alper, M., Karaagac, O., Hacıismailoglu, M., “Electrodeposited Ni–Co films from electrolytes with different Co contents”, *Appl. Surf. Sci.* 2012, 258, 4005–4010.
 19. Tsyntsar, N., Cesiulis, H., Pellicer, E., Celis, J. P. and Sort, J., “Structural, magnetic, and mechanical properties of electrodeposited cobalt–tungsten alloys: Intrinsic and extrinsic interdependencies”, *Electrochim. Acta* 2013, 104, 94–103.
 20. Lallemand, F., Ricq, L., Deschaseaux, E., De Vettor, L., Bercot, P., “Electrodeposition of cobalt–iron alloys in pulsed current from electrolytes containing organic additives”, *Surface & Coatings Technology* 2005, 197, 10–17
 21. Qiang, C., Xu, J., Xiao, S., Jiao, Y., Zhang, Z., Liu, Y., Tian, L. and Zhou, Z., “The influence of pH and bath composition on the properties of Fe–Co alloy film electrodeposition”, *Appl. Surf. Sci.* 2010, 257, 1371–1376.
 22. Cullity, B. D., Stock, S. R., Stock, S., “Elements of X-ray Diffraction”, Addison-Wesley, London, 2001.
 23. Hassani, Sh., Raeissi, K. and Golozar, M. A., “Effects of saccharin on the electrodeposition of Ni–Co nanocrystalline coatings”, *J. Appl. Electrochem.* 2008, 38, 689–694.
 24. Ghaferi, Z., Raeissi, K., Golozar, M. A. and Edris, H., “Characterization of nanocrystalline Co–W coatings on Cu substrate, electrodeposited from a citrate–ammonia bath”, *Surf. Coat. Technol.* 2011, 206, 497–505.
 25. Ghaferi, Z., Sharafi, S. and Bahrololoom, M. E., “The role of electrolyte pH on phase evolution and magnetic properties of CoFeW codeposited films”, *Appl. Surf. Sci.* 2016, 375, 35–41.
 26. Tian, L., Xu, J., Xiao, S., “The influence of pH and bath composition on the properties of Ni–Co coatings synthesized by electrodeposition”, *Vacuum* 2011, 86, 27–33.
 27. Oriňáková, R., Oriňák, A., Vering, G., Talian, I., Smith, R. M. and Arlinghaus, H. F., “Influence of pH on the electrolytic deposition of Ni–Co films”, *Thin Solid Films* 2008, 516, 3045–3050.
 28. Farzaneh, M. A., Zamanzad-Ghavidel, M. R., Raeissi, K., Golozar, M. A., Saatchi, A., Kabi, S., “Effects of Co and W alloying elements on the electrodeposition aspects and properties of nanocrystalline Ni alloy coatings”, *Appl. Surf. Sci.* 2011, 257, 5919–5926.
 29. Pavithra, G. P., Chitharanjan Hegde, A., “Magnetic property and corrosion resistance of electrodeposited nanocrystalline iron–nickel alloys”, *Appl. Surf. Sci.* 2012, 258, 6884–6890.
 30. Farzaneh, M. A. Raeissi, K., Golozar, M. A., “Effect of current density on deposition process and properties of nanocrystalline Ni–Co–W alloy coatings”, *J. Alloys Compd.* 2010, 489, 488–492.
 31. Fathollahzade, N., Raeissi, K., “Electrochemical evaluation of corrosion and tribocorrosion behavior of amorphous and nanocrystalline cobalt–tungsten electrodeposited coatings”, *Mater. Chem. Phys.* 2014, 148, 67–76.
 32. Nakahara, S., Mahajan, S., the influence of solution pH on microstructure of electrodeposited cobalt, *J. Electrochem. Soc.* 1980, 127, 283–288.
 33. Cohen-Hyams, T., Kaplan, W. D., Yahalom, J., “Structure of electrodeposited cobalt”, *Electrochem. Solid State Lett.* 2002, 5(8), C75–C78.
 34. He, F., Yang, J., Lei, T. and Gu, C., “Structure and properties of electrodeposited Fe–Ni–W alloys with different levels of tungsten content: A comparative study”, *Appl. Surf. Sci.* 2007, 253, 7591–7598.
 35. Nasirpour, F., Sanaeian, M. R., Samardak, A. S., Sukovatitsina, E. V., Ognev, A. V., Chebotkevich, L. A., Hosseini, M. G., Abdolmaleki, M., “An investigation on the effect of surface morphology and crystalline texture on corrosion behavior, structural and magnetic properties of electrodeposited nanocrystalline nickel films”, *Appl. Surf. Sci.* 2014, 292, 795–805.
 36. Sanaty-Zadeh, A., Raeissi, K. and Saidi, A.,

- “Properties of nanocrystalline iron–nickel alloys fabricated by galvanostatic Electrodeposition”, *J. Alloys Compd.* 2009, 485, 402–407.
37. Yun, H. J., Dulal, S. M. S. I., Shin, C. B. and Kim, C. K., “Characterisation of electrodeposited Co–W–P amorphous coatings on carbon steel”, *Electrochim. Acta* 2008, 54, 370–375.
38. Wang, L., Gao, Y., Xu, T. and Xue, Q., “A comparative study on the tribological behavior of nanocrystalline nickel and cobalt coatings correlated with grain size and phase structure”, *Mater. Chem. Phys.* 2006, 99, 96–103.
39. Su, F. h. and Huang, P., “Microstructure and tribological property of nanocrystalline Co–W alloy coating produced by dual-pulse electrodeposition”, *Mater. Chem. Phys.* 2012, 134, 350– 359.
40. Cullity, B. D. and Graham, C. D., “Introduction to magnetic materials”, John Wiley & Sons, 2011
41. Bahrami, A. H., Sharafi, S., Ahmadian Baghbaderani, H., “The effect of Si addition on the microstructure and magnetic properties of permalloy prepared by mechanical alloying method”, *Adv. Powder Technol.* 2013, 24, 235–241.
42. Khajepour, M. and Sharafi, S., “Structural and magnetic properties of nanostructured Fe₅₀(Co₅₀)–6.5 wt% Si powder prepared by high energy ball milling”, *J. Alloys Compd.* 2011, 509, 7729–7737.
43. Sharifati, A. and Sharafi, S., “Structure and magnetic properties of mechanically alloyed (Fe₇₀Co₃₀)₉₁Cu₉ powder”, *Mater. Design* 2012, 36, 35–40.
44. Zuo, B., Saraswati, N., Sriharan, T. and Hng, H. H., “Production and annealing of nanocrystalline Fe–Si and Fe–Si–Al alloy powders”, *Mater. Sci. Eng. A* 2004, 371, 210–216.
45. Ahmadian Baghbaderani, H., Sharafi, S. and Delshad Chermahini, M., “Investigation of nanostructure formation mechanism and magnetic properties in Fe₄₅Co₄₅Ni₁₀ system synthesized by mechanical alloying”, *Powder Technol.* 2012, 230, 241–246.
46. Karpuz, A., Kockar, H. and Alper, M., The effect of different chemical compositions caused by the variation of deposition potential on properties of Ni–Co films, *Appl. Surf. Sci.* 2011, 257, 3632–3635.
47. Sakita, A. M. P., Passamani, E. C., Kumar, H., Cornejo, D. R., Fugivara, C. S., Noce, R. D. and Benedetti, A. V., “Influence of current density on crystalline structure and magnetic properties of electrodeposited Co-rich CoNiW alloys”, *Materials Chemistry and Physics* 2013, 141, 576–581.